IAES International Journal of Robotics and Automation (IJRA)
Vol. 15, No. 1, March 2026, pp. 171~180
ISSN: 2722-2586, DOI: 10.11591/ijra.v15i1.pp171-180

Vibration control of semi-active suspension system using super-twisting sliding mode controller

Liuding Sun[1], Siti Azfanizam Ahmad[1], Jun Kit Ong[1], Suhadiyana Hanapi[2], Azizan As'arry[1]
[1]Department of Mechanical and Manufacturing Engineering, Faculty of Engineering, Universiti Putra Malaysia, Serdang, Malaysia
[2]Mechanical Engineering Studies, College of Engineering, Universiti Teknologi MARA, Shah Alam, Malaysia

Article Info

Article history:

Received Apr 9, 2025
Revised Nov 16, 2025
Accepted Dec 15, 2025

Keywords:

Chattering problem
Magnetorheological damper
Semi-active suspension
Super-twisting sliding mode controller
Vibration

ABSTRACT

The development of suspension systems arises from the impact of vehicle vibrations caused by road irregularities on passengers. Among various suspension systems, semi-active suspension (SAS) is favored for its cost-effectiveness and power efficiency. Magnetorheological (MR) dampers are commonly used in SAS to enhance vibration control by adjusting the magnetic field. However, the traditional sliding mode control (SMC) method often causes chattering, which affects performance. This study proposes the application of a super-twisting sliding mode controller (STSMC) to improve vibration control in SAS and overcome the chattering problem. Simulations and experimental evaluations were conducted on a quarter-car test bench with different road excitations. The results show that the STSMC-based system outperforms the traditional controller in vibration suppression. Specifically, the suppression effect on the root mean square value of body acceleration on a sinusoidal road surface can reach up to 38.2%. Therefore, the STSMC controller demonstrates superior vibration control in SAS systems equipped with MR dampers, providing a valuable reference for future research on SAS vibration control.

This is an open access article under the CC BY-SA license.

Corresponding Author:

Siti Azfanizam Ahmad
Department of Mechanical and Manufacturing Engineering, Faculty of Engineering,
Universiti Putra Malaysia
43400 Serdang, Selangor, Malaysia
Email: s_azfanizam@upm.edu.my

1. INTRODUCTION

Numerous studies have shown that prolonged exposure to high-intensity vibrations not only causes discomfort but also increases the risk of physical pain and musculoskeletal disorders, which are significant contributors to health problems [1]. To mitigate these effects, vehicle suspension systems are designed as mechanical devices to reduce the transmission of vibrations to the human body, which often originates from sources such as road irregularities caused by bumps or obstacles [2], [3].

To address the challenges associated with vibration control, advancements in suspension technology have focused on improving energy efficiency and system simplicity while maintaining effective vibration mitigation [4]. As an energy control component, actuators can either add or dissipate energy within the system as required. However, such systems are inherently complex and involve significantly higher energy consumption, particularly for the force actuators utilized within the system [5], [6]. Semi-active suspension (SAS) utilizes multiple sensors to determine the appropriate type and magnitude of damping force required, without relying on an external power source [7], [8]. SAS is recognized for its cost-effectiveness and power efficiency, while still delivering performance comparable to that of active suspension systems [9]–[12]. As a result, it has been extensively studied to enhance vehicle stability and handling performance [13]–[16].

Magnetorheological (MR) dampers are widely used in semi-active suspension systems due to their rapid response and capability to operate effectively at high temperatures [17], [18]. The magnetorheological fluid (MRF) within the damper can adjust the damping force in response to variations in the magnetic field [19]. By employing appropriate control strategies, semi-active suspensions can achieve vibration-damping performance comparable to active suspensions [20], [21].

Sliding mode control (SMC) demonstrates superior robustness in handling system characteristics such as uncertainties, disturbances, and fluctuations [22]. However, traditional SMC tends to induce chattering phenomena when the system undergoes frequent and rapid variations [23]. This phenomenon is characterized by high-frequency oscillations near the sliding surface caused by discontinuous switching control laws. Such chattering may lead to adverse effects, including increased wear of mechanical components, excitation of unmodeled high-frequency dynamics, and potential degradation of control performance [24]. The super-twisting sliding mode control (STSMC) method overcomes this issue without requiring adjustments to the controller, while still achieving the desired performance of the sliding mode control algorithm [25].

This study employs a super-twisting sliding mode controller to test and optimize the system's response under complex road excitations to enhance the vibration control performance of vehicle suspension systems. The focus is the design of a STSMC based on the mathematical model of the SAS for a quarter-vehicle. Additionally, the performance of different controllers is compared to assess their effectiveness. The content of this paper is organized as follows: Section 2 presents the methodology relevant to this study, including the schematic block diagram of the STSMC controller, the design of the STSMC controller, and the parameters of the experimental setup along with the design of experimental procedures. Section 3 presents experimental results, followed by a comprehensive analysis and discussion in both the time and frequency domains. Section 4 summarizes the key findings of this study and discusses the potential applications and future extensions of the proposed design methodology.

2. METHOD

2.1. STSMC controller system

This study proposes the STSMC controller and integrates it into a quarter-car semi-active suspension system to evaluate its performance in controlling the MR damper for vibration suppression. Figure 1 shows the block diagram of the super-twisting sliding mode control method applied to the MR damper.

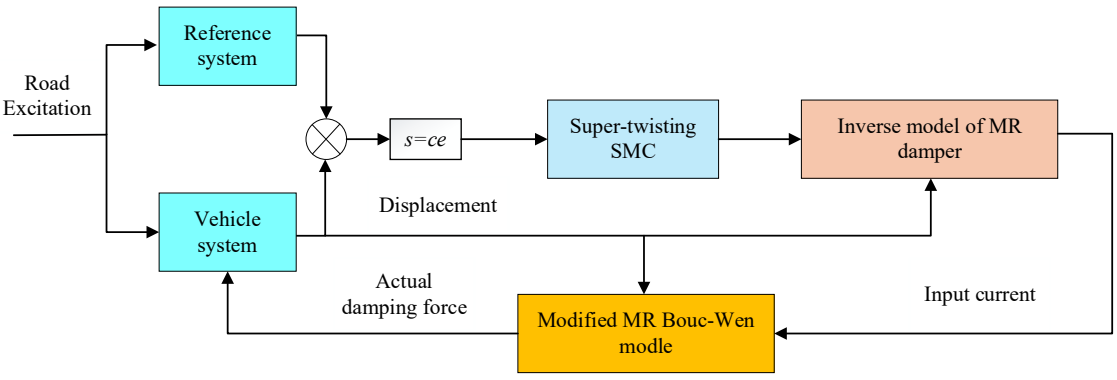

Figure 1. Schematic block diagram of STSMC controller

2.2. Design of STSMC controller

The control theory of STSMC introduces higher-order terms into the control signal. As with traditional SMC controllers, a sliding surface is first defined, as shown in (1), and its derivative is presented in (2).

$$s = e_2 + \lambda e_1 \quad (1)$$

$$\dot{s} = \dot{e_2} + \lambda e_2 \quad (2)$$

The primary difference between traditional SMC controllers and STSMC controllers lies in replacing the discontinuous component of the control force with a continuous second-order derivative term, as proposed by Wang *et al.* [26]. This improved approach achieves smoother control action while preserving the robustness and finite-time convergence properties of traditional SMC. Building upon this foundation, Soosairaj and Kandavel [27] incorporated the super-twisting algorithm into the STSMC framework to further enhance performance. The super-twisting algorithm enables the system to reach and remain on the sliding surface without requiring information about the derivative of the sliding variable. The equivalent control is defined as shown in (3) and (4).

$$F_{dc} = -k_1 * |s(t)|^{\frac{1}{2}} * sign\big(s(t)\big) + v \tag{3}$$

$$\dot{v} = -k_2 * sign\big(s(t)\big) \tag{4}$$

The following equation governed the tracking error of the STSMC controller, $e = x_1 - x_{1d}$, where x_1 represented the actual sprung mass displacement while x_{1d} represented the desired sprung mass displacement. The ideal Skyhook controller serves as the reference model for the STSMC controller. The force required to suppress vibrations is calculated using the tracking error, based on the first-order differential equation of the sliding surface function, as seen in (2). The control force, F_d, calculated from the STSMC controller, is governed by the following equation: $F_d = F_{eq} + F_{dc}$, where F_{eq} represents the equivalent control force used to guide the system toward the sliding surface, and F_{dc} represents the switching control force employed to maintain the system's state on the sliding surface. Additionally, the controller design ensures $\dot{V}(s) \leq 0$, in compliance with the Lyapunov stability theorem [17]. The control force F_d calculated is given by (5).

$$F_d = m_s\lambda\dot{e}(t) + \left[-k_s e - c_s\dot{e} + f_{sky}\right] - k_1 * |s(t)|^{\frac{1}{2}} * sign\big(s(t)\big) - \int k_s sign(s(t) \tag{5}$$

The rheological characteristics of the MR damper can only be adjusted by modifying the input voltage, which alters the magnetic field, thereby affecting the rheological characteristics. In this context, Soosairaj and Kandavel [27] proposed a voltage control strategy specifically designed to regulate the input voltage supplied to the MR damper. Their approach allows for real-time adaptation of the damper's performance based on system demands. The control technique they introduced is illustrated below, with the control parameters set as G =0.75 and B =1.5, which determine the responsiveness and scaling behavior of the voltage regulation mechanism.

$$\begin{aligned}
&if\ G(F_d - B * F_{MR}) * sgn(F_{MR}) > Vmax\\
&then, v = Vmax\\
&else\ if\ G(F_d - B * F_{MR}) * sgn(F_{MR}) < Vmin\\
&then\ v = Vmin\\
&else\\
&v = \ G(F_d - B * F_{MR}) * sgn(F_{MR})
\end{aligned}$$

2.3. Experimental setup

The experiment was conducted on a quarter-car suspension test rig equipped with a SAS system featuring an MR damper. The quarter-car model consisted of a frame chassis, an MR damper, an LVDT, a Dunlop tyre with 155/70 R12 dimensions, and upper and lower double wishbone A-arms. The damper used was the LORD RD-8041-1 MR damper, a long-stroke, semi-active device capable of delivering controllable damping force through the application of a magnetic field. This model is widely recognized for its reliability and performance in vibration control applications, making it well-suited for use in semi-active suspension systems.

The test rig also featured a shaker used to generate the required road excitation, which was achieved through vertical reciprocating motion facilitated by a pneumatic cylinder mounted beneath the excitation plate. As illustrated in Figure 2, The experimental parameters are consistent with those used by Ahmed *et al*. [8]. The test rig enables experimental evaluations by providing an accurate representation of the conceptual design of a SAS system [28].

The first part of the experiment is to verify the impact of STSMC on chatter vibration. The performance and dynamic quality of the SMC are influenced by the algorithms applied to it [29]. Therefore, the simulation compared the chattering effects of the traditional SMC, exponential SMC (ESMC), and STSMC under different road profiles. Table 1 presents the test control algorithms and parameters used in this

section. These parameters were determined through iterative simulation experiments, aiming to optimize the system response and minimize chattering while maintaining stability under both sinusoidal and random excitations. Additionally, the responses of the sprung mass acceleration (SMA) and sprung mass displacement (SMD) on the quarter-car suspension test rig were analyzed to investigate the impact of STSMC on passenger comfort.

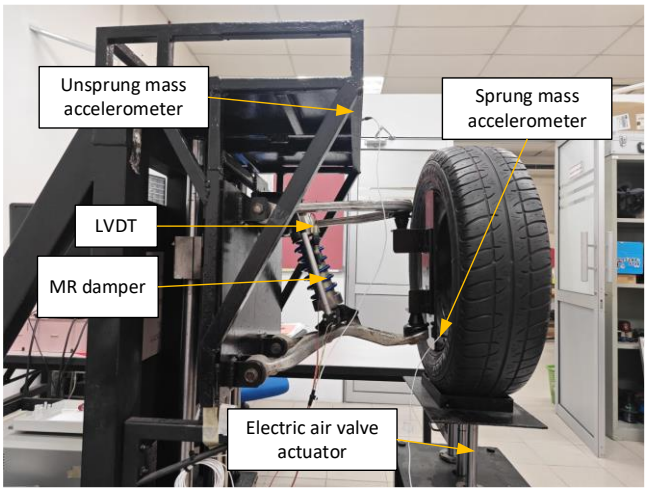

Figure 2. Quarter-car test rig setup

Table 1. Control algorithms and parameters used for SMC controller

Sliding mode control algorithm	Control function	Parameters
Conventional	$F_{d,sw} = -k \cdot sgn(s)\ ;\ (k > 0)$	k=98
Exponential	$\dot{s} = -ks - \varepsilon \cdot sgn(s)\ ;$ $(k > 0\ and\ \varepsilon > 0)$	k=98 ε= 0.005
Super-twisting	$v = -k_1\sqrt{\lvert s\rvert} \cdot sgn(s) + g\ ;\ (k_1 > 0)$ $g = -\int k_2 \cdot sgn(s)\ ;\ (k_2 > 0)$	k_1 =20 k_2 =0.005

The second part of the experiment is to evaluate the effectiveness of STSMC on suspension vibrations. In this section, a 10 kg inherent weight was placed on the sprung mass to simulate the load, and the performance of both simulation and experiment was tested under a 6 mm amplitude sinusoidal road profile. The performance of the STSMC controller was then compared with that of the uncontrolled passive system and the semi-active suspension system. The uncontrolled MR damper operated with a constant input voltage of 1 V, maintaining consistent damping characteristics throughout both the experimental and simulation processes.

3. RESULTS AND DISCUSSION

3.1. Suppression of chatter vibration by STSMC

Figure 3 illustrates the time-domain responses of the SMA under two types of road excitations: sinusoidal in Figure 3(a) and random in Figure 3(b), each evaluated under different sliding mode controllers. These subfigures are grouped together to provide a comparative view of SMA response performance under different excitation conditions, thereby forming a complete and comparable experimental analysis. The STSMC exhibited the smallest SMA amplitude (depicted by the solid blue line) and demonstrated reduced oscillations and a smoother response curve.

Additionally, Table 2 indicates that the root mean square (RMS) values of the STSMC controller decreased by 1.47% and 7.71% under sinusoidal and random road profiles, respectively. The reduction in RMS under random disturbances is particularly notable compared to the traditional SMC, which can be attributed to the robustness of the super-twisting algorithm in handling uncertainties. Moreover, the peak-to-peak (PTP) values under sinusoidal and random profiles were further reduced by 3.17% and 6.00%, respectively, compared to the traditional SMC.

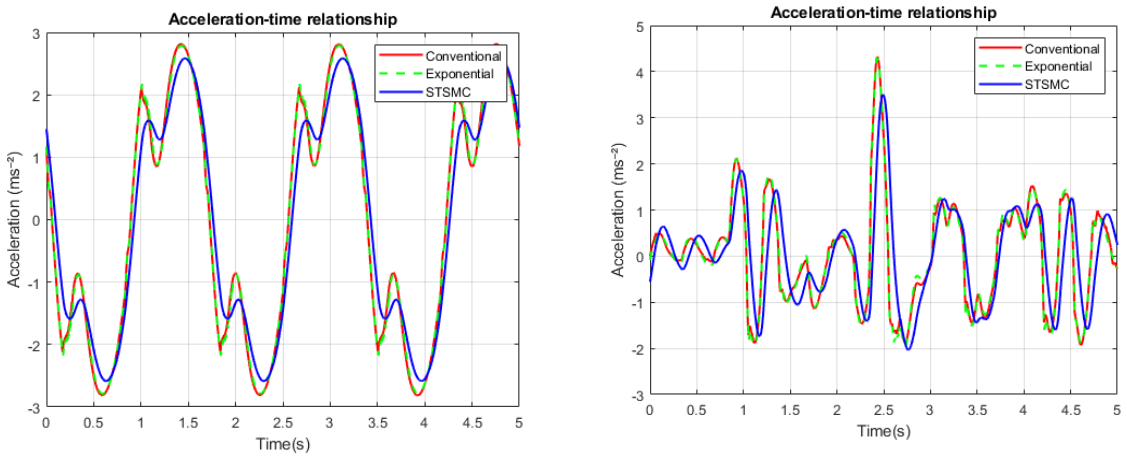

Figure 3. The time-domain SMA response of the SMC controller under (a) sinusoidal input and (b) random input

Table 2. Performance comparison between conventional SMC and STSMC controlled-MR damper under different road profiles

Road profile	Method	Performance indices	Conventional SMC	Reduction (%)	
				Exp-SMC	STSMC
Sinusoidal	RMS	SMA (m/s^2)	1.9079	0.37	1.47
	PTP	SMA (m/s^2)	5.5923	0.84	3.17
Random	RMS	SMA (m/s^2)	1.4816	0.01	7.71
	PTP	SMA (m/s^2)	8.2112	0.08	6.00

3.2. Control effectiveness of suspension vibrations

Figure 4 presents the time-domain responses of the system under sinusoidal road excitation, where Figure 4(a) shows the response curve of the SMA and Figure 4(b) shows that of the SMD. These two subfigures are jointly used to evaluate the vibration suppression performance of the STSMC controller from two complementary perspectives—ride comfort and suspension working space—under identical excitation and control conditions. Their combination enables a more comprehensive assessment of the controller's effectiveness in the time domain.

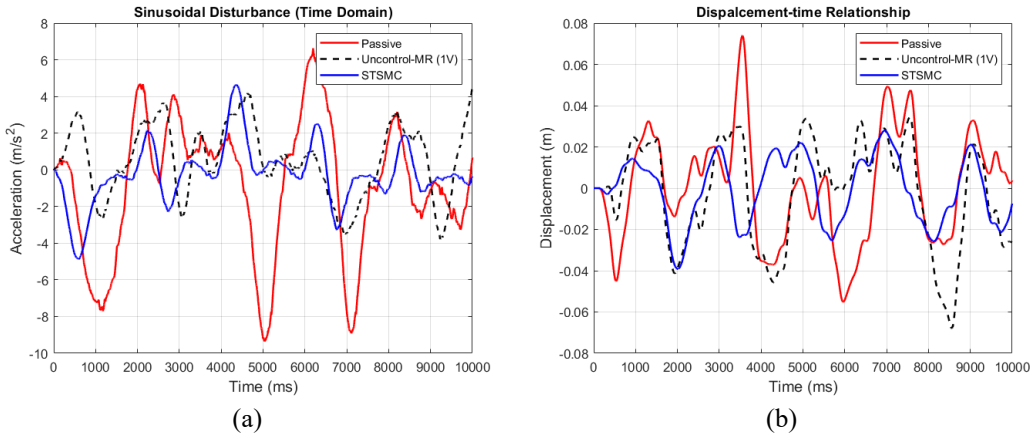

Figure 4. Time domain responses of (a) SMA and (b) SMD under sinusoidal road excitation

Figure 5 further analyses the system response characteristics from a frequency-domain perspective, where Figure 5(a) presents the spectral response of the SMA and Figure 5(b) shows that of the Unsprung mass acceleration (USMA). These two subfigures reflect the effectiveness of STSMC in suppressing the

acceleration energy distribution of different vehicle body components. The results show that STSMC significantly reduces the system's energy output in both the dominant and high-frequency regions, further confirming its superior control performance and stability in both time and frequency domains.

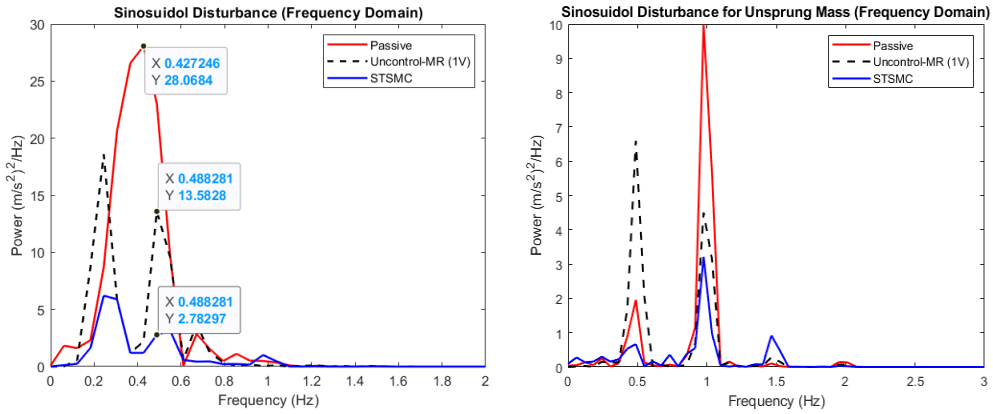

(a) (b)

Figure 5. Frequency domain responses of (a) SMA and (b) USMA under sinusoidal road excitation

Figures 6 and 7 present the time-domain and frequency-domain responses of the system obtained from the experiment, aiming to comprehensively evaluate the performance of the STSMC control strategy under realistic, non-ideal excitations. Figures 6(a) and 6(b) show the SMA and the SMD, respectively. These subfigures are grouped under a single figure number to jointly assess the time-domain vibration suppression performance from both acceleration and displacement perspectives under the same excitation and control conditions. Figures 7(a) and 7(b) display the spectral responses of the SMA and the USMA, respectively. They are combined under one figure number to facilitate a systematic frequency-domain comparison of energy distribution across different parts of the vehicle body.

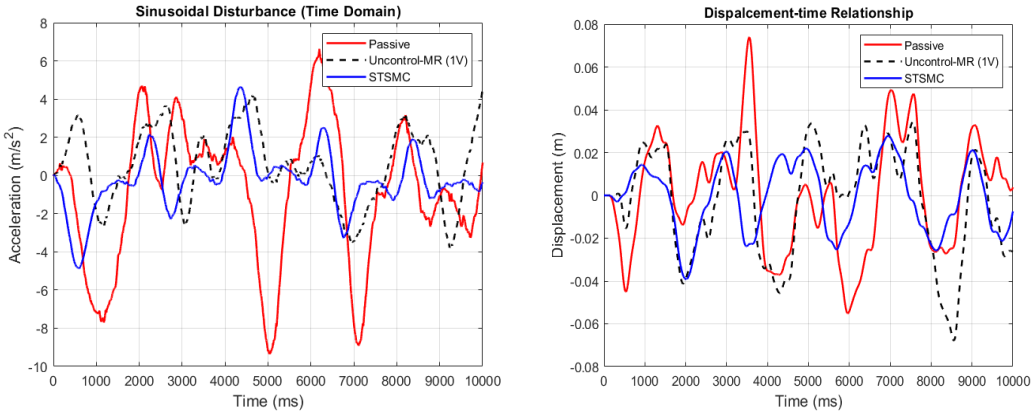

(a) (b)

Figure 6. Time-domain responses of the (a) SMA and (b) SMD under sinusoidal road conditions in the experiment

The experimental results demonstrate that the STSMC controller outperforms both the uncontrolled MR system and the passive system across multiple performance indicators, including reduced response amplitudes, diminished fluctuations, and suppressed high-frequency energy. The results in both the time and frequency domains are consistent with each other. In particular, the STSMC achieves significant improvements in controlling the SMA response, reducing peak amplitudes by approximately 27% in simulation and 33% in experiment. These findings are broadly consistent with those reported by Piwowarczyk *et al*. [23].

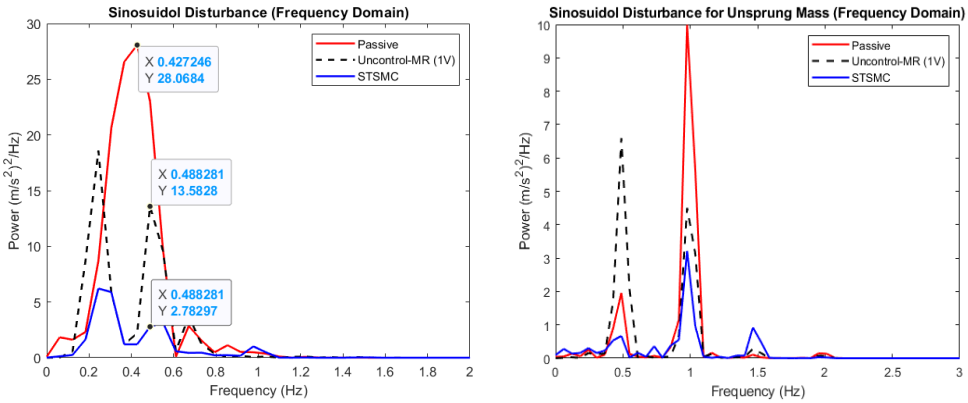

(a) (b)

Figure 7. Frequency-domain responses of the (a) SMA and (b) SMD under sinusoidal road conditions in the experiment

Both the simulation and experimental results indicate that the proposed STSMC controller exhibits outstanding performance in vibration suppression and system stability enhancement, leading to a significant improvement in the performance of the SAS system. Moreover, a comparison of Figures 5 and 7 illustrates that in the frequency domain, there is a discrepancy in the SMA natural frequency between the simulation and experiment, as the behavior of the physical system in the actual environment differs from the ideal conditions assumed in the simulation. However, the frequencies obtained in both the simulation and experiment fall within the natural frequency range (0-2 Hz) of commercial passenger vehicle suspension systems [30].

To quantitatively evaluate the vibration suppression performance of the proposed STSMC controller, both the RMS and PTP values of the SMA were calculated. Table 3 presents the RMS and PTP results for all three amplitudes of SMA in both simulation and experiment. The results indicate that compared to the passive and uncontrolled MR dampers, the RMS and PTP values for the STSMC controller show a decreasing trend. For example, the RMS value for the uncontrolled MR damper was 0.9798 m/s², while for the STSMC-controlled MR damper, it decreased to 0.8549 m/s², representing a reduction of 22.3%. This indicates that the STSMC controller significantly reduces the vibration intensity of the system, thereby enhancing its stability and comfort.

Table 3. Comparison of the vehicle's body acceleration RMS (m/s^2) during simulation and experiment on sinusoidal road profile

Statistical measures	Result	Passive	Uncontrolled- MR (1 Volt)	STSMC	Reduction (%)	
					Un-MR	STSMC
RMS (m/s^2)	Simulation	0.9676	0.8315	0.6682	14.1	30.9
	Experiment	1.1007	0.9798	0.8549	11.0	22.3
PTP (m/s^2)	Simulation	2.9910	2.6207	1.9983	12.4	33.2
	Experiment	4.6834	4.3215	3.8956	7.7	16.8

4. CONCLUSION

In conclusion, the STSMC significantly reduces chattering, achieving a smoother response curve and demonstrating considerable stability under varying load conditions. Compared to passive systems and uncontrolled MR dampers, the STSMC-controlled SAS system equipped with MR dampers outperforms both within the frequency range of 0 to 2 Hz, with vibration suppression reaching up to 38.2%.

This study proposes an STSMC strategy and, for the first time, applies it to the experimental validation of a quarter-car suspension system actuated by a MR damper. Both simulation and experimental results demonstrate the significant advantages of this control approach in vibration suppression. The integration of STSMC with the MR damper effectively reduces vibration exposure for drivers and passengers, thereby lowering potential health risks. The findings offer valuable insights into future research and practical applications in automotive suspension control.

However, this study is based on a quarter-car suspension model, which, while effective for preliminary validation, limits direct applicability to full-vehicle dynamics. Future work will extend the proposed control strategy to a full-vehicle suspension model to further explore practical implementation.

ACKNOWLEDGMENTS

The authors would like to thank Universiti Putra Malaysia (UPM) and the Malaysian Ministry of Higher Education (MOHE) for their continuous support in the research work.

FUNDING INFORMATION

This work was supported in part by the Geran Putra Inisiatif (GPI) fund (GPI/2024/9794100).

AUTHOR CONTRIBUTIONS STATEMENT

This journal uses the Contributor Roles Taxonomy (CRediT) to recognize individual author contributions, reduce authorship disputes, and facilitate collaboration.

Name of Author	C	M	So	Va	Fo	I	R	D	O	E	Vi	Su	P	Fu
Liuding Sun	✓	✓	✓	✓	✓	✓		✓	✓	✓	✓		✓	
Siti Azfanizam Ahmad	✓	✓			✓		✓		✓	✓	✓	✓	✓	✓
Jun Kit Ong		✓		✓				✓						
Suhadiyana Hanapi		✓		✓				✓						
Azizan As'arry	✓						✓		✓	✓		✓		✓

C : **C**onceptualization
M : **M**ethodology
So : **So**ftware
Va : **Va**lidation
Fo : **Fo**rmal analysis
I : **I**nvestigation
R : **R**esources
D : **D**ata Curation
O : Writing - **O**riginal Draft
E : Writing - Review & **E**diting
Vi : **Vi**sualization
Su : **Su**pervision
P : **P**roject administration
Fu : **Fu**nding acquisition

CONFLICT OF INTEREST STATEMENT

Authors state no conflict of interest.

INFORMED CONSENT

We have obtained informed consent from all individuals included in this study.

DATA AVAILABILITY

The data that support the findings of this study are available on request from the corresponding author, S. A. Ahmad. The data, which contain information that could compromise the privacy of research participants, are not publicly available due to certain restrictions.

REFERENCES

[1] M. Bovenzi, M. Schust, and M. Mauro, "An overview of low back pain and occupational exposures to whole-body vibration and mechanical shocks," *La Medicina del Lavoro*, vol. 108, no. 6, pp. 419–433, Dec. 2017, doi: 10.23749/mdl.v108i6.6639.

[2] J. Yang *et al.*, "A semi-active suspension using a magnetorheological damper with nonlinear negative-stiffness component," *Mechanical Systems and Signal Processing*, vol. 147, p. 107071, Jan. 2021, doi: 10.1016/j.ymssp.2020.107071.

[3] A. As'Arry, F. M. Naseer, T. A. Z. Rahman, K. A. M. Rezali, and M. Z. M. Zain, "Semi-active suspension control for formula SAE car using magneto-rheological fluid," in *2017 IEEE Symposium on Computer Applications & Industrial Electronics (ISCAIE)*, Apr. 2017, pp. 97–101, doi: 10.1109/ISCAIE.2017.8074957.

[4] D. Shetty and M. Allen, "A parametric study of the Bouc–Wen model for bolted joint dynamics," *Journal of Vibration and Acoustics*, vol. 145, no. 4, p. 041004, Aug. 2023, doi: 10.1115/1.4062103.

[5] S. S. Eligar and R. M. Banakar, "A Survey on passive, active and semiactive automotive suspension systems and analyzing tradeoffs in design of suspension systems," in *2018 International Conference on Recent Innovations in Electrical, Electronics & Communication Engineering (ICRIEECE)*, Jul. 2018, pp. 2908–2913, doi: 10.1109/ICRIEECE44171.2018.9008620.

[6] J. Sun, J. Cong, W. Zhao, and Y. Zhang, "Quantized feedback control of active suspension systems based on event trigger," *Shock and Vibration*, vol. 2021, no. 1, pp. 1–15, Jan. 2021, doi: 10.1155/2021/8886069.

[7] A. Soliman and M. Kaldas, "Semi-active suspension systems from research to mass-market – a review," *Journal of Low Frequency Noise, Vibration and Active Control*, vol. 40, no. 2, pp. 1005–1023, Jun. 2021, doi: 10.1177/1461348419876392.

[8] H. Ahmed, A. As'arry, A. A. Hairuddin, M. Khair Hassan, Y. Liu, and E. C. U. Onwudinjo, "Online DE optimization for fuzzy-PID controller of semi-active suspension system featuring MR damper," *IEEE Access*, vol. 10, pp. 129125–129138, 2022, doi: 10.1109/ACCESS.2022.3196160.

[9] M. Rahman, Z. C. Ong, W. T. Chong, S. Julai, and R. Ahamed, "Experimental investigation of nonlinear characteristics of a smart fluid damper," in *AIP Conference Proceedings*, 2018, p. 020031, doi: 10.1063/1.5034562.
[10] K. El Majdoub, D. Ghani, F. Giri, and F. Z. Chaoui, "Adaptive semi-active suspension of quarter-vehicle with magnetorheological damper," *Journal of Dynamic Systems, Measurement, and Control*, vol. 137, no. 2, p. 021010, Feb. 2015, doi: 10.1115/1.4028314.
[11] Z. Wang, C. Liu, X. Zheng, L. Zhao, and Y. Qiu, "Advancements in semi-active automotive suspension systems with magnetorheological dampers: a review," *Applied Sciences*, vol. 14, no. 17, p. 7866, Sep. 2024, doi: 10.3390/app14177866.
[12] D. N. Nguyen and T. A. Nguyen, "The dynamic model and control algorithm for the active suspension system," *Mathematical Problems in Engineering*, vol. 2023, no. 1, p. 2889435, Jan. 2023, doi: 10.1155/2023/2889435.
[13] G. Q. B. Tran, T.-P. Pham, O. Sename, E. Costa, and P. Gaspar, "Integrated comfort-adaptive cruise and semi-active suspension control for an autonomous vehicle: an LPV approach," *Electronics*, vol. 10, no. 7, p. 813, Mar. 2021, doi: 10.3390/electronics10070813.
[14] A. Gupta, N. Bharadwaj, and V. Rastogi, "Computational framework of various semi-active control strategies for road vehicles thorough bondgraphs," *International Journal of System Dynamics Applications*, vol. 10, no. 4, pp. 1–29, Jul. 2021, doi: 10.4018/IJSDA.20211001.oa9.
[15] A. M. A. Soliman, "Effect of road disturbance on the ride performance of twin accumulator and semi-active suspension systems," Mar. 2017, doi: 10.4271/2017-01-0410.
[16] S. Fazeli and A. Moarefianpur, "An adaptive approach for vehicle suspension system control in presence of uncertainty and unknown actuator time delay," *Systems Science & Control Engineering*, vol. 9, no. 1, pp. 117–126, Jan. 2021, doi: 10.1080/21642583.2020.1850369.
[17] K. Zizouni, A. Saidi, L. Fali, I. K. Bousserhane, and M. Djermane, "Semi-active structural vibration control with magnetorheological damper based on hybrid fuzzy sliding mode controller," *IAES International Journal of Robotics and Automation (IJRA)*, vol. 12, no. 2, p. 167, Jun. 2023, doi: 10.11591/ijra.v12i2.pp167-178.
[18] A. Masa'id, B. W. Lenggana, U. Ubaidillah, D. D. Susilo, and S.-B. Choi, "A review on vibration control strategies using magnetorheological materials actuators: application perspective," *Actuators*, vol. 12, no. 3, p. 113, Mar. 2023, doi: 10.3390/act12030113.
[19] G. Hu, Q. Liu, R. Ding, and G. Li, "Vibration control of semi-active suspension system with magnetorheological damper based on hyperbolic tangent model," *Advances in Mechanical Engineering*, vol. 9, no. 5, p. 168781401769458, May 2017, doi: 10.1177/1687814017694581.
[20] G. Li, Z. Ruan, R. Gu, and G. Hu, "Fuzzy sliding mode control of vehicle magnetorheological semi-active air suspension," *Applied Sciences*, vol. 11, no. 22, p. 10925, Nov. 2021, doi: 10.3390/app112210925.
[21] H. Zambare, A. Khoje, S. Patil, and A. Razban, "MR damper modeling performance comparison including hysteresis and damper optimization," *IEEE Access*, vol. 9, pp. 24560–24569, 2021, doi: 10.1109/ACCESS.2021.3057174.
[22] L. Ovalle, H. Ríos, and H. Ahmed, "Robust control for an active suspension system via continuous sliding-mode controllers," *Engineering Science and Technology, an International Journal*, vol. 28, p. 101026, Apr. 2022, doi: 10.1016/j.jestch.2021.06.006.
[23] M. Piwowarczyk, M. Sibielak, and J. Konieczny, "Semi-active vehicle suspension with SMC controller," in *2023 24th International Carpathian Control Conference (ICCC)*, Jun. 2023, pp. 337–340, doi: 10.1109/ICCC57093.2023.10178971.
[24] J. Yao, W. Shi, J. Zheng, and H. Zhou, "Development of a sliding mode controller for semi-active vehicle suspensions," *Journal of Vibration and Control*, vol. 19, no. 8, pp. 1152–1160, Jun. 2013, doi: 10.1177/1077546312441045.
[25] G. V. Hollweg, P. J. D. de O. Evald, D. M. C. Milbradt, R. V. Tambara, and H. A. Gründling, "Design of continuous-time model reference adaptive and super-twisting sliding mode controller," *Mathematics and Computers in Simulation*, vol. 201, pp. 215–238, Nov. 2022, doi: 10.1016/j.matcom.2022.05.014.
[26] T. Wang, S. Chen, H. Ren, and Y. Zhao, "State estimation and damping control for unmanned ground vehicles with semi-active suspension system," *Proceedings of the Institution of Mechanical Engineers, Part D: Journal of Automobile Engineering*, vol. 234, no. 5, pp. 1361–1376, Apr. 2020, doi: 10.1177/0954407019881022.
[27] A. S. Soosairaj and A. Kandavel, "Ride comfort analysis of driver seat using super twisting sliding mode controlled magnetorheological suspension system," *Proceedings of the Institution of Mechanical Engineers, Part D: Journal of Automobile Engineering*, vol. 235, no. 14, pp. 3606–3618, Dec. 2021, doi: 10.1177/09544070211008763.
[28] P. Swethamarai and P. Lakshmi, "Design and implementation of fuzzy-PID controller for an active quarter car driver model to minimize driver body acceleration," in *2019 IEEE International Systems Conference (SysCon)*, Apr. 2019, pp. 1–6, doi: 10.1109/SYSCON.2019.8836940.
[29] T. Tang, S. Sha, C. Pan, and H. Li, "Sliding mode control of vehicle semi-active suspension system based on magnetorheological damper," *Journal of Physics: Conference Series*, vol. 2459, no. 1, p. 012085, Mar. 2023, doi: 10.1088/1742-6596/2459/1/012085.
[30] M. Adhar Bagus, A. As'arry, H. A. Abdul Mutaleb Abas, A. A. Hairuddin, and M. K. Hassan, "Vibration control of FSAE quarter car suspension test rig using magnetorheological damper," *Indonesian Journal of Electrical Engineering and Computer Science (IJEECS)*, vol. 17, no. 3, p. 1281, Mar. 2020, doi: 10.11591/ijeecs.v17.i3.pp1281-1288.

BIOGRAPHIES OF AUTHORS

Liuding Sun was born in Luoyang, China. He received his bachelor's degree in automation from Lanzhou Jiaotong University in 2019 and is currently pursuing a master's degree from Universiti Putra Malaysia. His research interests include control system theory, neural networks and optimization algorithms. He can be contacted at Liudingsun@outlook.com.

Siti Azfanizam Ahmad is an associate professor of department of mechanical and manufacturing engineering, faculty of engineering at Universiti Putra Malaysia (UPM), Serdang, Malaysia. Her education includes a Ph.D. (manufacturing engineering) from Cardiff University, UK, and a BS. systems engineering from University of Arizona, USA. Her research interest is in swarm-based algorithm, optimization and TRIZ. She can be contacted at s_azfanizam@upm.edu.my.

Ong Jun Kit was born in Johor, Malaysia. He received the bachelor's degrees in mechanical engineering from Universiti Putra Malaysia, Malaysia, in 2021. He is currently a quality engineer at Texas Instruments Malaysia (TIM), Malaysia. He can be contacted at Junkit101001@gmail.com.

Suhadiyana Hanapi was a senior lecturer in the college of engineering (mechanical), Universiti Teknologi MARA, Cawangan Johor, Kampus Pasir Gudang. She received her PhD from Universiti Teknologi MARA (UiTM) in 2017. Her research interests include PEM fuel cell, electric vehicles, renewable energy and intelligent optimization. She can be contacted at suhadiyana@uitm.edu.my.

Azizan As'arry was born in Kuala Lumpur, Malaysia. He received the bachelor's, master's, and Ph.D. degrees in mechanical engineering from Universiti Teknologi Malaysia, Malaysia, in 2007, 2009, and 2013, respectively. His major field of study is control and mechatronics. He is currently a Senior Lecturer at Universiti Putra Malaysia, Malaysia. His research interests include active force control, system identification, system modeling, and simulation. He can be contacted at zizan@upm.edu.my.